

Integral Membrane Protein Fragment Recombination after Transfer from Nanolipoprotein Particles to Bicelles

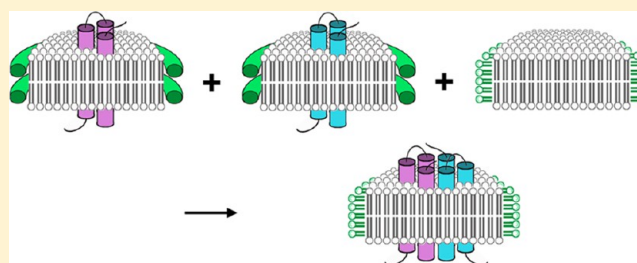
Ginny Lai[†] and Robert Renthal^{*,†,‡}

[†]Department of Biology, University of Texas at San Antonio, San Antonio, Texas 78249, United States

[‡]Department of Biochemistry, University of Texas Health Science Center at San Antonio, San Antonio, Texas 78229, United States

S Supporting Information

ABSTRACT: A new method for the measurement of membrane protein oligomer association is described. Two engineered fragments of bacteriorhodopsin, which are known to spontaneously associate in bicelles, were expressed in nanolipoprotein particles (NLPs or nanodiscs) using an *Escherichia coli* S30 cell-free synthesis system. When separately prepared NLPs containing the fragments were mixed, fragment association did not occur, indicating that the apolipoprotein edge blocks transfer between NLPs. However, when bicelles were added to this mixture, fragment association was detected by disulfide cross-linking. The rate of cross-linking was consistent with previously published equilibrium and kinetic parameters. Characterization of the NLP/bicelle mixture by dynamic light scattering and fluorescence spectroscopy indicates that the NLP bilayer transfers to bicelles in a simple reversal of the synthesis of NLPs from bicelles. These experiments validate using cell-free synthesis of membrane proteins in NLPs, followed by treatment with bicelles, as a method for measuring oligomerization of integral membrane protein subunits in a bilayer-like environment.



Many integral membrane proteins, including channels, transporters, and enzymes, consist of subunits that associate into oligomers. Regulation of hetero-oligomeric membrane protein formation may be an important mechanism of modulating activity.^{1–3} However, there are no general methods for studying the assembly of oligomeric membrane proteins *in vitro*. Unlike water-soluble protein oligomers that can usually be dissociated by dilution, membrane protein oligomers in vesicles typically do not dissociate because of the limited membrane area.⁴ Although detergent micelles have been used as an environment for the analysis of membrane protein oligomerization thermodynamics,⁵ in some cases association constants are much lower in micelles than in bilayers.⁶ Thus, it would be valuable to have bilayer systems for studies of association equilibria and assembly pathways of oligomeric membrane proteins. A suitable system would have to contain protomers in a monomeric state, but it would also have to release the protomers under experimental control.

Nanolipoprotein particles (NLPs), also known as nanodiscs, are small lipid bilayer patches bounded by apolipoprotein chains.^{7,8} NLPs form spontaneously when apolipoproteins are added to liposomes⁹ or when detergent monomers are removed from a mixture of detergent-solubilized lipids and apolipoproteins.¹⁰ If integral membrane proteins are included in the detergent/lipid mixture, NLPs that contain embedded integral membrane proteins are produced.¹¹ Protein oligomers in detergent micelles become surrounded by the NLP structure during the removal of detergent. Thus, monomers of oligomeric membrane proteins are not observed in NLPs

prepared in this manner.^{12,13} NLPs have been used in cell-free synthesis of integral membrane proteins.¹⁴ In this method, the number of protein molecules inserted into each NLP can be varied from one to multiple copies, depending on the relative cross-sectional areas of the proteins and NLPs,¹⁴ and probably also depending on other factors such as the ribosome concentration and turnover. Proteins embedded in NLPs may be prevented from moving between NLPs because the membrane edges are sealed by the apolipoprotein belt (Figure 1A). If so, then it may be possible to find conditions that open NLPs for mixing that could be used to control the assembly of oligomeric membrane proteins. Bicelles are lipid/detergent mixtures that form bilayer disks similar to NLPs at low lipid:detergent ratios. Unlike NLPs, bicelle edges are in rapid equilibrium with detergent monomers (Figure 1B), suggesting that they could be used to fuse with and open NLPs. This process would simply be the reverse of the method used to synthesize NLPs from cholate, lipids, and apolipoprotein.⁷ In this paper, we test the idea that NLP-embedded membrane protein protomers can be associated under controlled conditions using bicelles, thereby providing a new method for studying the oligomerization of membrane proteins. We utilize two engineered fragments of bacteriorhodopsin (bR) [bR-S, containing two transmembrane helices, and bR-L, containing

Received: February 28, 2013

Revised: December 13, 2013

Published: December 13, 2013

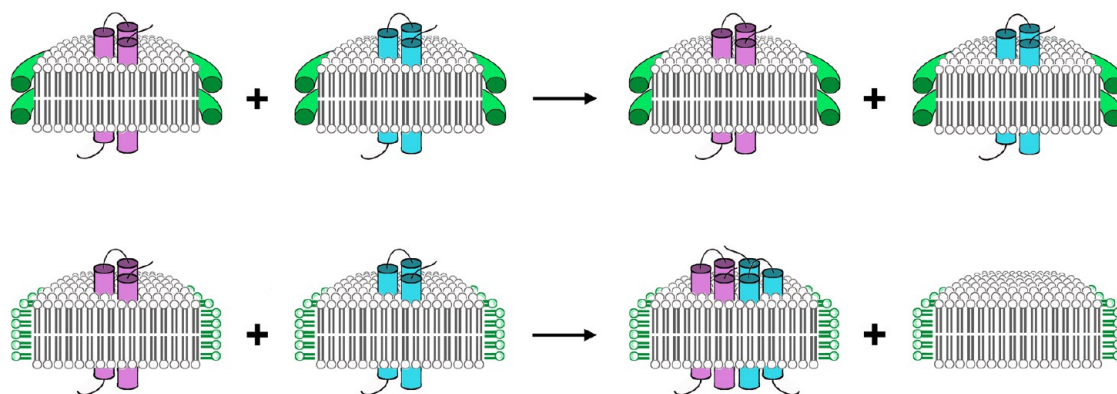


Figure 1. Model membranes: NLPs and bicelles. In the top row, nanolipoprotein particles (NLPs) are bilayer patches bounded by apolipoproteins that prevent the exchange of integral membrane proteins, so monomers cannot form oligomers. In the bottom row, bicelles are bilayer patches bounded by rings of short chain lipids. They can exchange integral membrane proteins, permitting oligomerization.

five transmembrane helices (Figure 2)] that are known to spontaneously associate in bicelles.^{15,16}

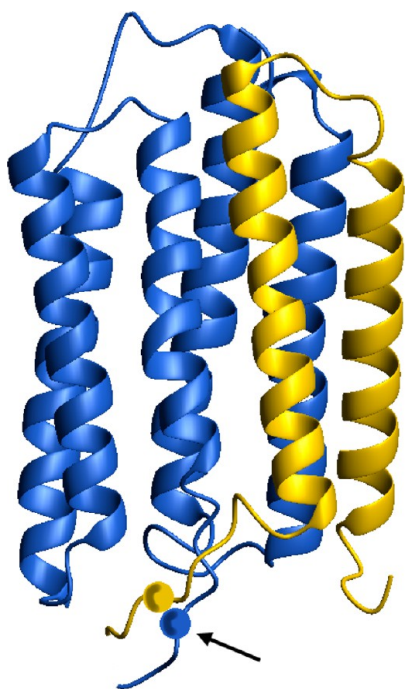


Figure 2. Fragments of bR. bR-S is colored yellow (amino acids 1–71) and bR-L blue (amino acids 1–8 and 72–248). Engineered Cys residues M68C and Q75C (spheres) form a disulfide cross-link (arrow) under oxidizing conditions. This figure was generated with bR coordinates from Protein Data Bank entry 1C3W using MOLMOL.³⁵

MATERIALS AND METHODS

Bacteriorhodopsin Fragments. DNA sequences corresponding to two chymotrypsin fragments of bR [bR-S (amino acids 1–71) and bR-L (amino acids 1–8 and 72–248)] were generated by polymerase chain reaction. Fragment bR-S is identical to what was previously called C-2¹⁷ or AB,¹⁸ and bR-L is similar to C-1,¹⁷ CDEFG,¹⁹ or CG.¹⁸ Fragments bR-S and bR-L also contained an N-terminal Met. For cross-linking experiments, fragment bR-S was engineered with an M68C mutation, designated bR-S(M68C), and fragment bR-L was engineered with a Q75C mutation, designated bR-L(Q75C).

Fragments were separately cloned into pEXP5-CT/TOPO vectors (Invitrogen, Carlsbad, CA) and expressed by cell-free co-transcriptional/translational synthesis using an *Escherichia coli* S30 system with added NLPs (100 μ L MembraneMax Protein Expression Kit, Invitrogen), following the manufacturer's instructions. Typical yields of bR fragments in the cell-free expression reaction were in the range of 1–3 μ M, as quantified by Western blotting (see below). The corresponding NLP concentration was in the range of 6.3–7.6 μ M, according to information provided by Invitrogen.

Cross-Linking Reactions. Bicelle stock solutions were prepared from 272 mM 1,2-dihexanoyl-*sn*-glycero-3-phosphocholine (DHPC) and either 204 or 272 mM 1,2-dimyristoyl-*sn*-glycero-3-phosphocholine (DMPC) (Avanti Polar Lipids, Inc., Alabaster, AL) for a DMPC:DHPC mole ratio (q) of 0.75 or 1.0, respectively. In cross-linking experiments, 36 μ L of each of the two bR fragment/NLP products was mixed with 8 μ L of a bicelle stock solution and allowed to equilibrate at room temperature for 30 min. Cross-linking was initiated in 10 μ L aliquots by adding 2 μ L of a 12.8 mM CuSO₄/12.8 mM *o*-phenanthroline mixture for varying times. Cross-linking reactions were stopped by adding 5 μ L of a 6.3 M acrylamide/10 mM ethylenediaminetetraacetic acid mixture. The fragments and cross-linked products were separated by polyacrylamide gel electrophoresis and detected by Western blotting, using an anti-C-terminal six-His tag antibody (Invitrogen) conjugated to alkaline phosphatase, horseradish peroxidase, or fluorescein. Substrates were 5-bromo-4-chloro-3'-indolyl phosphate (SigmaFAST BCIP/NBT, Sigma-Aldrich, St. Louis, MO) for phosphatase or acridium ester (Pierce ECL 2 Western Blotting Substrate, Thermo Scientific, Rockford, IL) for peroxidase. Chromogenic blots were imaged with a digital camera, and chemiluminescence or fluorescein emission was imaged with a Typhoon scanner (GE Healthcare Biosciences, Piscataway, NJ). The amount of protein in each band was quantified by comparison of the band intensity with that of a standard His-tagged protein at a known concentration. The correction curve, which was fit with a logistic function, is given in Figure S1 of the Supporting Information.

NLP Preparation. *E. coli* BL21(DE3) cells were transformed with plasmid pMSP1E3D1 (Addgene, Cambridge, MA), which encodes MSP, the NLP scaffold apolipoprotein. MSP was expressed and purified by a method similar to that of Ritchie et al.¹⁰ Approximately 9 mg of MSP was obtained per liter of culture. DMPC, cholate (Sigma-Aldrich), and MSP were

mixed in a molar ratio of 80:160:1 and cycled between room temperature and 30 °C as described by Katzen et al.¹⁴ NLPs were formed by dialysis against phosphate-buffered saline to remove cholate.²⁰ The dialyzed NLPs (~1.5 mL) were applied to a 1.5 cm × 85 cm column of Sepharose 4B (Sigma-Aldrich). NLPs eluted in a broad peak centered at an apparent molecular mass of 260 kDa (calibrated with thyroglobulin, aldolase, and bovine serum albumin). The peak fractions had NLP concentrations of ~4 μM (assuming two MSP molecules per NLP). To measure lipid exchange, some NLPs were prepared with a mixture of DMPC and the fluorescent lipids 14:0-NBD-PE [1,2-dimyristoyl-*sn*-glycerol-3-phosphoethanolamine-*N*-(7-nitro-2-1,3-benzoxadiazol-4-yl)] and 14:0-LR-PE [1,2-dimyristoyl-*sn*-glycerol-3-phosphoethanolamine-*N*-(lissamine rhodamine B sulfonyl)] (Avanti Polar Lipids). The DMPC:NBD-PE:LR-PE:cholate:MSP mole ratio for the fluorescent NLP preparation was 73.8:3.1:3.1:160:1. In the purified fluorescent NLPs, the LR-PE:NBD-PE mole ratio obtained was ~4:1.

Dynamic Light Scattering. Particle size distributions of bicelles, NLPs, and bicelles with NLPs were measured at 25 °C on a Malvern Instruments (Worcestershire, U.K.) Zetasizer Nano ZS instrument, using a 12 μL cuvette. Conversion from spherical to ellipsoidal particle dimensions was calculated using Perrin factors,²¹ assuming the DMPC bilayer thickness is 4.34 nm.²²

Transfer of Protein between Bicelles and NLPs. The exchange of protein between bicelles was tested with bR-S and bR-L prepared from the *Halobacterium salinarum* purple membrane as described previously.^{15,23,24} Bicelles were prepared from 2% DMPC and 2% DHPC ($q = 0.67$). Separate 1.9 nmol samples of purified bR-S and bR-L in a 1:1 chloroform/methanol mixture and 0.1 M ammonium acetate were added to 20 μL of 2% sodium dodecyl sulfate and vacuum-dried. Each residue was solubilized in 100 μL of 0.05 M phosphate buffer (pH 6.0). One pair of bR-S/bR-L samples was mixed together, and then 75 μL bicelles were added. A second pair of bR-S/bR-L samples were separately added to 37.5 μL bicelles and equilibrated for 10 min before they were combined. To each bR-S/bR-L pair was added 1 μL of all-*trans*-retinal (0.75 mg/mL in ethanol) to regenerate the chromophore. Absorbance spectra were measured on an Aviv/Cary 14 spectrophotometer (Aviv Biomedical, Inc., Lakewood, NJ).

Transfer of Lipid between NLPs and Bicelles. The exchange of lipid between NLPs and bicelles was measured using the fluorescence resonance energy transfer method of Struck et al.²⁵ NLPs containing LR-PE and NBD-PE (see above) were suspended at a concentration of ~0.12 μM in buffer, buffer containing 250 μM NLPs lacking fluorescent lipids, or buffer containing DMPC/DHPC bicelles ($q = 1.0$; 136 mM DMPC). Fluorescence emission spectra were recorded in a 10 μL cuvette (10.10B, NSG Precision Cells, Inc., Farmingdale, NY) on a PTI QM-4 fluorometer (Photon Technology International, Birmingham, NJ).

RESULTS

Cell-Free Expression of bR Fragments in NLPs. Cell-free expression of integral membrane proteins in NLPs appeared to offer a suitable method for obtaining monomeric protomers for oligomerization studies, because expression conditions can be arranged to have either zero or one protein molecule inserted per NLP.^{8,14} However, cell-free expression places constraints on how oligomer formation can be detected, because oligomer yields may be <1 μM. Thus, we chose to

detect oligomers by using disulfide bond cross-linking, which can be measured on Western blots of nonreducing electrophoresis gels. When bacteriorhodopsin fragments bR-S and bR-L associate, they can be disulfide cross-linked by suitably placed cysteine residues. Examination of the crystal structure shows that the β-carbons of Met 68 and Gln 75 are within 4.5 Å (Figure 2), close to the distance of 4 Å often found in disulfide bonds. Therefore, we expect associated bR-S(M68C) and bR-L(Q75C) will be cross-linked under oxidizing conditions (Cu²⁺-phenanthroline). We found that both bR fragments were efficiently expressed in an *E. coli* S30 cell-free system containing NLPs (Figure 3, lanes 4 and 5). However,

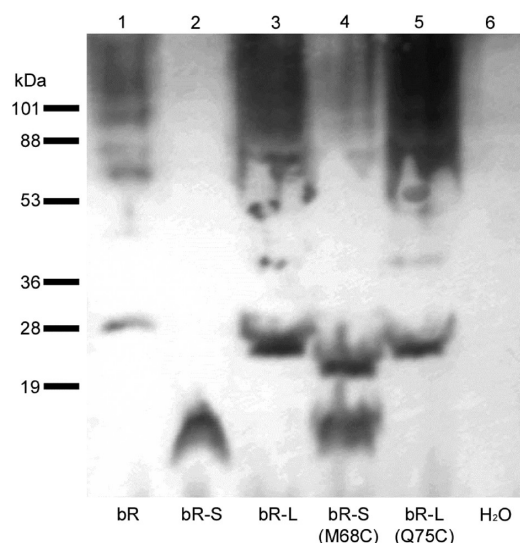


Figure 3. Expression of full-length bR and its fragments. Western blot of *E. coli* S30 cell-free synthesis products in the presence of NLPs, probed with the anti-six-His tag antibody: lane 1, full-length bR; lane 2, bR-S; lane 3, bR-L; lane 4, bR-S(M68C); lane 5, bR-L(Q75C). The formation of dimers occurred in cysteine-engineered bR-S(M68C) (lane 4), but not in bR-S (lane 2). Nonspecific binding appeared in both bR-L (lane 3) and cysteine-engineered bR-L(Q75C) (lane 5). Lane 6 (a negative control) contained H₂O.

approximately half of each protein appeared in higher-molecular mass forms on dodecyl sulfate gels. Dimerization occurred with bR-S(M68C) (Figure 3, lane 4). The dimers were disulfide cross-linked because dimerization was not observed in bR-S lacking cysteine (Figure 3, lane 2). Aggregation occurred in both bR-L and bR-L(Q75C) (Figure 3, lanes 3 and 5), both with *E. coli* proteins in the cell-free extract and with itself to form dimers and trimers. Thus, the aggregation of the large fragment did not depend on cysteine. Under reducing conditions, the bR-S(M68C) dimers were reversed, but the bR-L(Q75C) aggregates were not (data not shown). It is not clear how the bR-S(M68C) dimers form. They could result from monomers separately being inserted into the same NLP, or monomers could cross-link between two different NLPs. The bR-S dimers would not necessarily prevent association between bR-S and bR-L. Liao et al.²⁶ showed that two five-helix fragments of bR (A–E and C–G) associate to form active bR.

Some membrane proteins synthesized in cell-free systems fail to insert into membranes (e.g., liposomes, NLPs, or micelles) and form insoluble precipitates.^{14,27,28} We tested bR-S and bR-L for the extent of NLP insertion by comparing the Western

blot band intensities of the cell-free synthesis products before and after a brief centrifugation (Figure 4). For bR-S, 99% of the

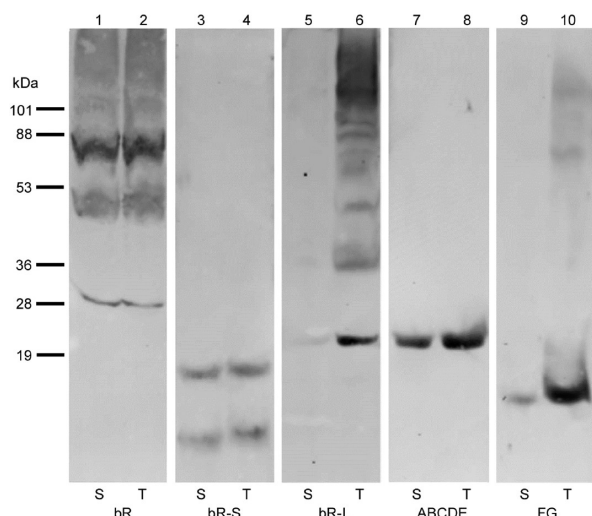


Figure 4. Extent of NLP insertion of full-length bR and its fragments. S, supernatant; T, total crude extract. bR fragments with N-terminal helices, including full-length bR (lanes 1 and 2), bR-S (lanes 3 and 4), and fragment ABCDE (lanes 7 and 8), showed more NLP insertion than bR-L (lanes 5 and 6) and fragment FG (lanes 9 and 10).

cell-free synthesis product was in the supernatant after centrifugation, indicating that it was efficiently inserted into NLPs (Figure 4, lanes 3 and 4). By contrast, only 37% of bR-L was inserted into NLPs (Figure 4, lanes 5 and 6). This result initially seemed puzzling because the NLP insertion efficiency of full-length bR was 99% (Figure 4, lanes 1 and 2). We also tested two additional bR fragments, one containing helices ABCDE [48% NLP insertion (Figure 4, lanes 7 and 8)] and another containing helices FG [32% NLP insertion (Figure 4, lanes 9 and 10)]. The results suggest that bR fragments containing the N-terminal helices, A and B, are more stable.

Transfer of Protein between NLPs and between Bicelles. When NLPs containing bR-S(M68C) were mixed with NLPs containing bR-L(Q75C), cross-linking between the fragments was not observed, either with or without addition of Cu^{2+} -phenanthroline (Figure 5, lanes 5 and 6). This indicates that the proteins could not move from one NLP to another, and the thiols were not accessible for cross-linking by collision between NLPs containing bR fragments.

To detect the exchange of protein between bicelles, we used bR-S and bR-L, which are known to form active bacteriorhodopsin after they associate in the presence of all-*trans*-retinal.^{15,17} In one experiment, bR-S and bR-L were mixed prior to the formation of bicelles. Addition of all-*trans*-retinal to this mixture generated a 550 nm chromophore (Figure 6, solid line), indicating that the two fragments had associated to form an active structure. In a second experiment, bR-S and bR-L were separately solubilized in bicelles and subsequently mixed together. After all-*trans*-retinal had been added to this mixture (Figure 6, dashed line), the amount of 550 nm pigment was 87% of the level measured from the two fragments starting in the same bicelle. This result shows that the separate fragments move rapidly from one bicelle to another, and this transfer process has an only weak effect on the process of subunit association that forms active structures.

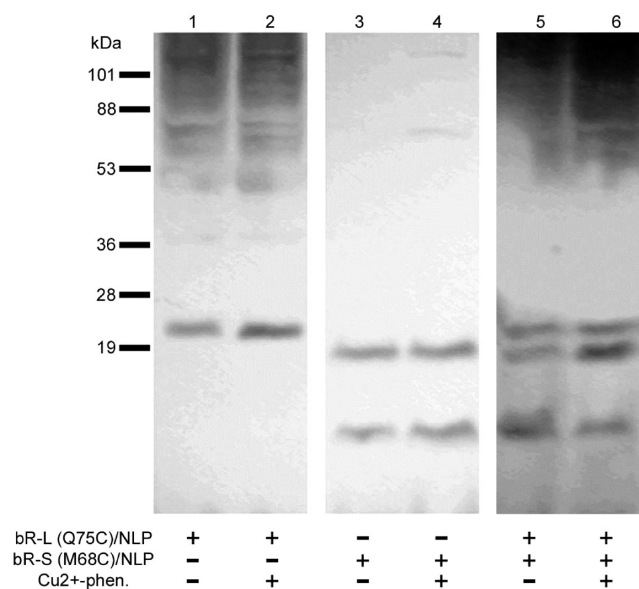


Figure 5. Proteins cannot transfer between NLPs. During synthesis in NLPs, bR-L(Q75C) (lanes 1 and 2) formed some cross-links with *E. coli* proteins, and bR-S(M68C) (lanes 3 and 4) dimerized. No cross-linking occurred after the addition of Cu^{2+} (lanes 2 and 4). When bR-L(Q75C) NLPs were mixed with bR-S(M68C) NLPs, no heteromers formed either without (lane 5) or with (lane 6) Cu^{2+} .

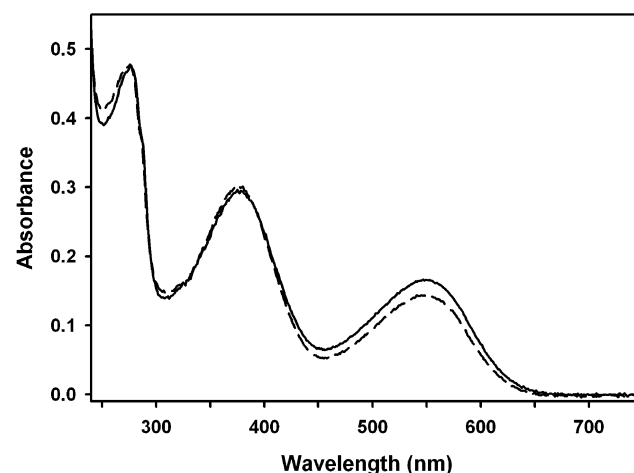


Figure 6. Membrane proteins spontaneously move between bicelles. Fragments bR-S and bR-L associated to form the active 550 nm pigment regardless of whether the fragments were mixed before (—) or after (---) the formation of DMPC/DHPC bicelles. The absorbance at 380 nm was due to excess all-*trans*-retinal.

Bicelles Remove Lipids from NLPs. Because NLPs can be formed from a mixture of apolipoprotein and bicelles via the removal of detergent,⁷ it seemed reasonable that the reverse process should also occur. The effect of adding bicelles to NLPs was tested in two ways. First, the particle sizes were measured by dynamic light scattering (Figure 7). The NLPs had a number-average radius of 6.5 nm, whereas the bicelles had a number-average radius of 3.4 nm. When NLPs and bicelles were mixed, the size distribution shifted to particles with a number-average radius of 4.3 nm. Previous analysis of NLPs by atomic force microscopy showed a distribution of discrete sizes, presumably because of specific apolipoprotein conformations. For ApoA1 and MSP, the smallest NLPs observed by

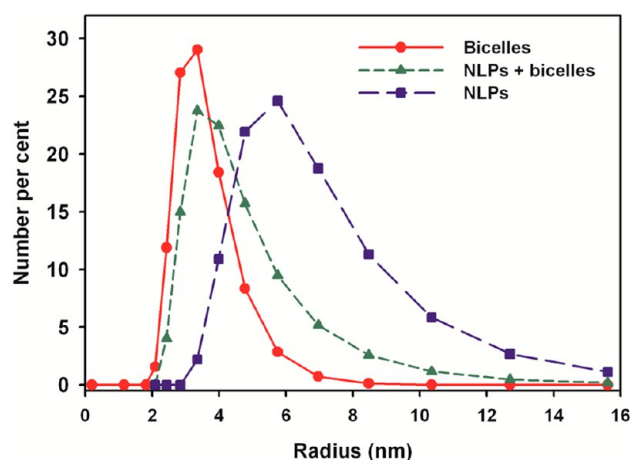


Figure 7. Dynamic light scattering of bicelles and NLPs. Circles with a solid line show data of bicelles ($q = 1.0$) containing 136 mM DMPC. Squares with a long-dash line show data of NLPs containing 12.6 μM MSP. Triangles with a short-dash line show data of a mixture of bicelles ($q = 1.0$; 27.2 mM DMPC) and NLPs (12.6 μM MSP).

Blanchette et al. had average radii of ~ 6.5 nm, and the next two larger sizes had radii of 8.5 and 11 nm.²⁹ Therefore, if DMPC is transferred from bicelles to NLPs, the maximal size distribution change would be expected to occur at radii from 8.5 to 11 nm. Figure 7 instead shows a broad increase in the numbers of particles with sizes from 5 to 8 nm. Clearly, the NLPs are not growing. Instead, it appears that the bicelles are growing, presumably by removing DMPC from NLPs.

A second study of the interaction of bicelles and NLPs was conducted using fluorescence spectroscopy. NLPs were prepared containing approximately nine LR-PE molecules and approximately two NBD-PE molecules, along with approximately 220 molecules of DMPC per surface. The emission spectrum of these NLPs (Figure 8, curve A) shows no emission from the NBD group, indicating that its fluorescence is quenched by strong Förster resonance energy transfer (FRET).

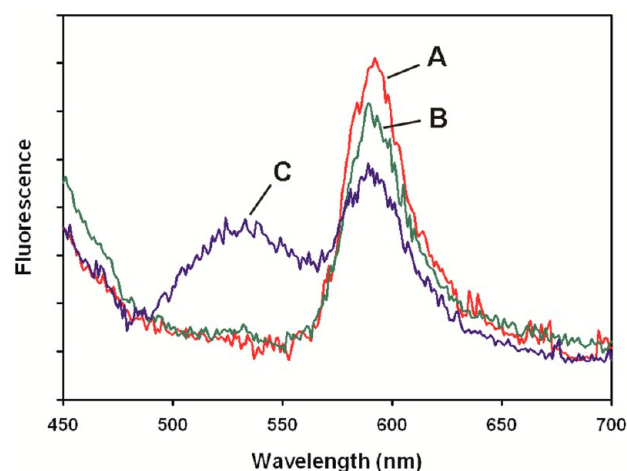


Figure 8. NLP and bicelle lipid mixing. (A) Fluorescent NLPs containing NBD-PE, LR-PE, and DMPC in an approximately 2:9:220 ratio. (B) Fluorescent NLPs mixed with an ~ 30 -fold excess of nonfluorescent NLPs. (C) Fluorescent NLPs mixed with DMPC/DHPC bicelles ($q = 1.0$; 136 mM DMPC). The excitation wavelength was 440 nm.

The same concentration of fluorescent NLPs was mixed with an approximately 30-fold excess of nonfluorescent NLPs. After equilibration at 25 $^{\circ}\text{C}$ for 50 min, the fluorescence emission spectrum was measured (Figure 8, curve B). A small amount of NBD emission was detected, along with an $\sim 13\%$ decrease in LR emission. This shows that NLPs are highly resistant to exchanging lipids. In a third sample, the same concentration of fluorescent NLPs was mixed with DMPC/DHPC bicelles ($q = 1.0$; 136 mM DMPC). After equilibration at 25 $^{\circ}\text{C}$ for 60 min, the fluorescence emission spectrum was measured (Figure 8, curve C). The spectrum now shows a strong emission band from NBD and $\sim 33\%$ decreased emission from LR. This indicates that in the presence of bicelles, the distance between NBD-PE energy donors and LR-PE energy acceptors increases. The results do not distinguish between bicelle lipids being absorbed into larger NLPs and bicelles extracting lipids from NLPs. However, in view of the light scattering measurements (Figure 7), it is more likely that DMPC/DHPC bicelles remove lipids from NLPs.

DMPC/DHPC Bicelles Promote the Association of NLP-Containing Membrane Proteins. Fragments bR-S(M68C) and bR-L(Q75C) in NLPs were mixed in the presence of DMPC/DHPC bicelles (Figure 9, lanes 3 and 4). When Cu^{2+} -phenanthroline was added (Figure 9, lane 4), a new band appeared (arrow), at the migration distance corresponding to intact bacteriorhodopsin (Figure 9, lane 7). Therefore, bicelles promote the transfer of membrane proteins out of NLPs and permit oligomers to form. Fewer oligomers were formed in the absence of Cu^{2+} -phenanthroline (Figure 9, lane 3), or with DHPC micelles alone (Figure 9, lanes 1 and 2).

Rate of Oligomer Formation Measured Using Cross-Linking Reaction. The appearance of cross-linked product (conditions of Figure 9, lane 4) was measured as a function of time (Figure 9 lanes 8–11). The initial velocities of the reaction were measured at two different ratios of bR-S(M68C) concentration to bR-L(Q75C) concentration (Figure 10), although the accuracy is limited by having only three points per curve. The amount of cross-linked product leveled off at a limiting value of ~ 0.25 μM . This appears to be a low yield of cross-linked product compared to the measured total concentrations of bR fragments [0.51 and 0.97 μM bR-S(M68C) and 0.95 and 1.1 μM bR-L(Q75C), neglecting the aggregated forms]. However, considering that only 37% of the total bR-L was inserted into NLPs, the maximal expected yield would be ~ 0.4 μM . Thus, the observed yield is $\sim 60\%$. Oxidative side reactions might also play a role in limiting the yield.

DISCUSSION

It is not clear how nascent membrane proteins are delivered from ribosomes into NLPs. There is no mechanism known for insertion of multispan integral membrane proteins into lipid bilayers in the absence of chaperones or translocons.³⁰ Although it is likely that the fragments of bR are embedded in the NLP bilayer, as intact bR was shown to be,¹⁴ we do not have direct evidence of this. We assume there are suitable chaperones in the *E. coli* S30 cell extract. It is possible that these chaperones can deliver newly synthesized membrane proteins to an NLP where they could be absorbed edgewise into the bilayer, one helix at a time, possibly through an interaction with the apolipoprotein belt. If this mechanism is correct, it would essentially be irreversible because once in the NLP bilayer, the protein would fold, resulting in a free energy barrier to leaving

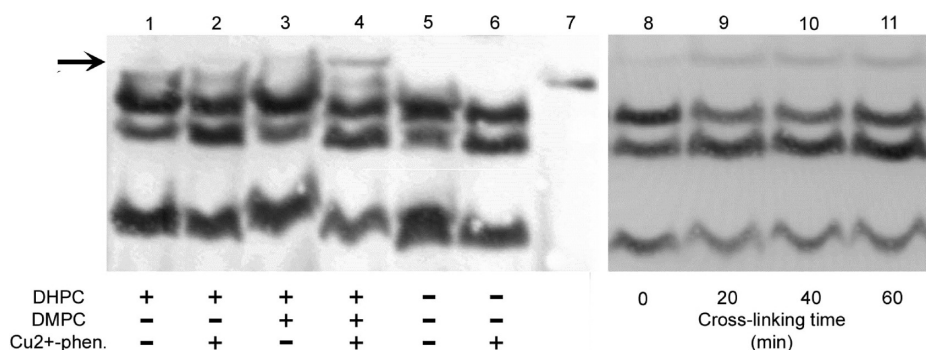


Figure 9. Bicelles promote the oligomerization of NLP-bound proteins. With added bicelles and Cu²⁺, the mixture of bR-S(M68C) NLPs and bR-L(Q75C) NLPs (lane 4) formed cross-links (arrow; cf. wild-type bR in lane 7), indicating opening of NLPs and association of fragments. Without Cu²⁺ (lanes 1, 3, and 5) or without bicelles (lanes 1, 2, 5, and 6), little or no fragment association occurred. Lanes 8–11 show cross-linking kinetics.

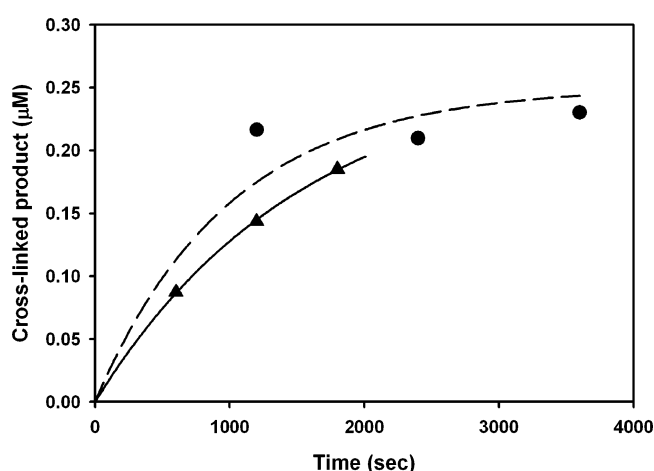


Figure 10. Cross-linking kinetics. The initial velocity of the cross-linking reaction between subunits in associated fragments is related to both the association constant for oligomer formation and the rate constant for disulfide formation (eq 4). Total initial protein concentrations: (▲) 0.51 μM bR-S(M68C) and 0.35 μM bR-L(Q75C) and (●) 0.97 μM bR-S(M68C) and 0.41 μM bR-L(Q75C). Lines are exponential growth curves used to estimate initial velocities.

the NLP. Our results show that monomeric integral membrane proteins in NLPs are restricted from associating into oligomers (Figure 5). We observed large differences in the yields of insertion of protein into NLPs. The bR fragments with the highest insertion yields all contained the two N-terminal helices. A previous study suggested that two or more N-terminal helices of bacteriorhodopsin are more stable than the C-terminal helices and may serve as a folding template.³¹

The addition of bicelles to NLP-embedded membrane proteins frees the monomers from the NLPs, permitting the transfer from one bicelle to another and the formation of oligomers (Figure 9). The mechanism for this appears to involve bicelles removing material from NLPs (Figures 7 and 8). A previous report suggested that planar bilayers can remove lipids and proteins from NLPs.¹³ However, the transfer was detected by single-channel conductance, which could have originated from a small subpopulation of non-NLP proteins.

We measured the association of two fragments of bR that are known to spontaneously assemble,¹⁶ using cross-linking between engineered cysteines. The rate of the cross-linking reaction contains information about the subunit association

constant, K_A . The cross-linking rate, V , is assumed to follow pseudo-first-order kinetics:³²

$$V = k_x[SL] \quad (1)$$

where k_x is the pseudo-first-order rate constant for cross-linking and $[SL]$ is the molar concentration of associated bR-S(M68C) and bR-L(Q75L). We assume that the fragments are in the $S + L \rightleftharpoons SL$ equilibrium. Therefore, association constant K_A is

$$K_A = [SL]/([S][L]) \quad (2)$$

where $[S]$ and $[L]$ are the molar concentrations of bR-S(M68C) and bR-L(Q75L), respectively. Thus, eq 1 can be rewritten as

$$V = k_x K_A [S][L] \quad (3)$$

Solving eq 3 for the initial velocity, V_o , gives

$$V_o = k_x K_A ([S_{t=0}]^2 - [S_{t=0}](S_T - L_T)) \quad (4)$$

where $[S_{t=0}]$ is the initial concentration of bR-S(M68C) and S_T and L_T are the total molar concentrations of bR-S(M68C) and bR-L(Q75C) in all their forms, respectively, excluding the aggregated forms (see the Supporting Information for the derivation of eq 4).

We substituted measured values into eq 4 for two different S_T/L_T ratios. With an L_T of 0.35 μM and an S_T of 0.51 μM, $[S_{t=0}] = 0.27$ μM and $V_o = 0.18$ nM/s. With an L_T of 0.41 μM and an S_T of 0.97 μM, $[S_{t=0}] = 0.63$ μM and $V_o = 0.25$ nM/s. Using a K_A of 7.7×10^6 M⁻¹¹⁶ and solving for k_x gives a value of 0.0007 s⁻¹ for both S_T/L_T ratios. This is in the range of k_x previously determined by Careaga and Falke³² for the formation of a disulfide between cysteine sulfur atoms separated by ~8 Å. From models, we found that the distance between the Sγ atoms of C68 and C75 could vary from 4.4 to 8.8 Å by rotation of the C-terminal sequence around the Ca–NH bond of C68 or rotation of the N-terminal sequence around the Ca–CO bond of C75. Thus, the methods reported here could be used, along with an independently measured cross-linking rate constant, to measure oligomer association constants (see eq S9 of the Supporting Information). In cases in which cross-linking is not feasible, oligomer formation after mixing membrane protein monomers in NLPs with bicelles could be monitored by FRET^{6,16} or other spectroscopic probes. Spectroscopic monitoring would also permit measurement of the rates of assembly of integral membrane protein oligomers. A particularly well-developed research area to which this new

method might be usefully applied is the homo- and hetero-oligomerization of G protein-coupled receptors.^{33,34}

CONCLUSION

Integral membrane protein monomers expressed in NLPs do not interact. However, controlled oligomerization can be achieved by adding DMPC/DHPC bicelles. This may be a useful method for investigating assembly rates and equilibria of oligomeric membrane proteins in a bilayer environment.

ASSOCIATED CONTENT

Supporting Information

Calibration curve for quantification of Western blots (Figure S1) and derivation of eq 4. This material is available free of charge via the Internet at <http://pubs.acs.org>.

AUTHOR INFORMATION

Corresponding Author

*Department of Biology, University of Texas at San Antonio, 1 UTSA Circle, San Antonio, TX 78249. E-mail: robert.renthal@utsa.edu. Telephone: (210) 458-5452.

Funding

This work was supported by a grant from the San Antonio Life Sciences Institute.

Notes

The authors declare no competing financial interest.

ACKNOWLEDGMENTS

We thank Kelly Nash for assistance with dynamic light scattering measurements, Qi Zhao for technical assistance, and Bruce Nicholson for helpful discussions.

ABBREVIATIONS

NLPs, nanolipoprotein particles; bR, bacteriorhodopsin; bR-S, bR amino acids 1–71 and the N-terminal methionine; bR-L, bR amino acids 1–8 and 72–248 with the N-terminal methionine; DMPC, 1,2-dimyristoyl-*sn*-glycero-3-phosphocholine; DHPC, 1,2-dihexanoyl-*sn*-glycero-3-phosphocholine; NBD-PE, 1,2-dimyristoyl-*sn*-glycerol-3-phosphoethanolamine-*N*-(7-nitro-2-1,3-benzoxadiazol-4-yl); LR-PE, 1,2-dimyristoyl-*sn*-glycerol-3-phosphoethanolamine-*N*-(lissamine rhodamine B sulfonyl); FRET, Förster resonance energy transfer.

REFERENCES

- (1) Koval, M. (2006) Pathways and control of connexin oligomerization. *Trends Cell Biol.* 16, 159–166.
- (2) Kumar, J., Schuck, P., and Mayer, M. L. (2011) Structure and assembly mechanism for heteromeric kainate receptors. *Neuron* 71, 319–331.
- (3) Valles, A. S., and Barrantes, F. J. (2012) Chaperoning $\alpha 7$ neuronal nicotinic acetylcholine receptors. *Biochim. Biophys. Acta* 1818, 718–729.
- (4) Hong, H., Blois, T. M., Cao, Z., and Bowie, J. U. (2010) Method to measure strong protein-protein interactions in lipid bilayers using a steric trap. *Proc. Natl. Acad. Sci. U.S.A.* 107, 19802–19807.
- (5) Fleming, K. G. (2002) Standardizing the free energy change of transmembrane helix-helix interactions. *J. Mol. Biol.* 323, S63–S71.
- (6) Kriegsmann, J., Brehs, M., Klare, J. P., Engelhard, M., and Fitter, J. (2009) Sensory rhodopsin II/transducer complex formation in detergent and in lipid bilayers studied with FRET. *Biochim. Biophys. Acta* 1788, 522–531.
- (7) Bayburt, T. H., and Sligar, S. G. (2010) Membrane protein assembly into Nanodiscs. *FEBS Lett.* 584, 1721–1727.

- (8) Chromy, B. A., Arroyo, E., Blanchette, C. D., Bench, G., Benner, H., Cappuccio, J. A., Coleman, M. A., Henderson, P. T., Hinz, A. K., Kuhn, E. A., Pesavento, J. B., Segelke, B. W., Sulchek, T. A., Tarasow, T., Walsworth, V. L., and Hoeprich, P. D. (2007) Different apolipoproteins impact nanolipoprotein particle formation. *J. Am. Chem. Soc.* 129, 14348–14354.
- (9) Wientzek, M., Kay, C. M., Oikawa, K., and Ryan, R. O. (1994) Binding of insect apolipoprotein III to dimyristoylphosphatidylcholine vesicles. Evidence for a conformational change. *J. Biol. Chem.* 269, 4605–4612.
- (10) Ritchie, T. K., Grinkova, Y. V., Bayburt, T. H., Denisov, I. G., Zolnerchik, J. K., Atkins, W. M., and Sligar, S. G. (2009) Chapter 11: Reconstitution of membrane proteins in phospholipid bilayer nanodiscs. *Methods Enzymol.* 464, 211–231.
- (11) Nath, A., Atkins, W. M., and Sligar, S. G. (2007) Applications of phospholipid bilayer nanodiscs in the study of membranes and membrane proteins. *Biochemistry* 46, 2059–2069.
- (12) Bayburt, T. H., Grinkova, Y. V., and Sligar, S. G. (2006) Assembly of single bacteriorhodopsin trimers in bilayer nanodiscs. *Arch. Biochem. Biophys.* 450, 215–222.
- (13) Banerjee, S., and Nimigean, C. M. (2011) Non-vesicular transfer of membrane proteins from nanoparticles to lipid bilayers. *J. Gen. Physiol.* 137, 217–223.
- (14) Katzen, F., Fletcher, J. E., Yang, J. P., Kang, D., Peterson, T. C., Cappuccio, J. A., Blanchette, C. D., Sulchek, T., Chromy, B. A., Hoeprich, P. D., Coleman, M. A., and Kudlicki, W. (2008) Insertion of membrane proteins into discoidal membranes using a cell-free protein expression approach. *J. Proteome Res.* 7, 3535–3542.
- (15) Liao, M. J., London, E., and Khorana, H. G. (1983) Regeneration of the native bacteriorhodopsin structure from two chymotryptic fragments. *J. Biol. Chem.* 258, 9949–9955.
- (16) Nannepaga, S. J., Gawalapu, R., Velasquez, D., and Renthal, R. (2004) Estimation of helix-helix association free energy from partial unfolding of bacteriorhodopsin. *Biochemistry* 43, 550–559.
- (17) Huang, K. S., Bayley, H., Liao, M. J., London, E., and Khorana, H. G. (1981) Refolding of an integral membrane protein. Denaturation, renaturation, and reconstitution of intact bacteriorhodopsin and two proteolytic fragments. *J. Biol. Chem.* 256, 3802–3809.
- (18) Marti, T. (1998) Refolding of bacteriorhodopsin from expressed polypeptide fragments. *J. Biol. Chem.* 273, 9312–9322.
- (19) Kahn, T. W., and Engelman, D. M. (1992) Bacteriorhodopsin can be refolded from two independently stable transmembrane helices and the complementary five-helix fragment. *Biochemistry* 31, 6144–6151.
- (20) Denisov, I. G., Grinkova, Y. V., Lazarides, A. A., and Sligar, S. G. (2004) Directed self-assembly of monodisperse phospholipid bilayer Nanodiscs with controlled size. *J. Am. Chem. Soc.* 126, 3477–3487.
- (21) Cantor, C. R., and Schimmel, P. R. (1980) *Biophysical Chemistry*, W. H. Freeman, San Francisco.
- (22) Kucerka, N., Tristram-Nagle, S., and Nagle, J. F. (2005) Structure of fully hydrated fluid phase lipid bilayers with monounsaturated chains. *J. Membr. Biol.* 208, 193–202.
- (23) Renthal, R., and Haas, P. (1996) Effect of transmembrane helix packing on tryptophan and tyrosine environments in detergent-solubilized bacterio-opsin. *J. Protein Chem.* 15, 281–289.
- (24) Sigrist, H., Wenger, R. H., Kislig, E., and Wuthrich, M. (1988) Refolding of bacteriorhodopsin. Protease V8 fragmentation and chromophore reconstitution from proteolytic V8 fragments. *Eur. J. Biochem.* 177, 125–133.
- (25) Struck, D. K., Hoekstra, D., and Pagano, R. E. (1981) Use of resonance energy transfer to monitor membrane fusion. *Biochemistry* 20, 4093–4099.
- (26) Liao, M. J., Huang, K. S., and Khorana, H. G. (1984) Regeneration of native bacteriorhodopsin structure from fragments. *J. Biol. Chem.* 259, 4200–4204.
- (27) Goren, M. A., and Fox, B. G. (2008) Wheat germ cell-free translation, purification, and assembly of a functional human stearyl-CoA desaturase complex. *Protein Expression Purif.* 62, 171–178.

- (28) Klammt, C., Schwarz, D., Fendler, K., Haase, W., Dotsch, V., and Bernhard, F. (2005) Evaluation of detergents for the soluble expression of α -helical and β -barrel-type integral membrane proteins by a preparative scale individual cell-free expression system. *FEBS J.* 272, 6024–6038.
- (29) Blanchette, C. D., Law, R., Benner, W. H., Pesavento, J. B., Cappuccio, J. A., Walsworth, V., Kuhn, E. A., Corzett, M., Chromy, B. A., Segelke, B. W., Coleman, M. A., Bench, G., Hoeprich, P. D., and Sulchek, T. A. (2008) Quantifying size distributions of nanolipoprotein particles with single-particle analysis and molecular dynamic simulations. *J. Lipid Res.* 49, 1420–1430.
- (30) Renthall, R. (2010) Helix insertion into bilayers and the evolution of membrane proteins. *Cell. Mol. Life Sci.* 67, 1077–1088.
- (31) Valluru, N., Silva, F., Dhage, M., Rodriguez, G., Alloor, S. R., and Renthall, R. (2006) Transmembrane helix-helix association: Relative stabilities at low pH. *Biochemistry* 45, 4371–4377.
- (32) Careaga, C. L., and Falke, J. J. (1992) Thermal motions of surface α -helices in the D-galactose chemosensory receptor. Detection by disulfide trapping. *J. Mol. Biol.* 226, 1219–1235.
- (33) Hiller, C., Kuhhorn, J., and Gmeiner, P. (2013) Class A G-protein-coupled receptor (GPCR) dimers and bivalent ligands. *J. Med. Chem.* 56, 6542–6559.
- (34) Mary, S., Fehrentz, J. A., Damian, M., Gaibelet, G., Orcel, H., Verdier, P., Mouillac, B., Martinez, J., Marie, J., and Baneres, J. L. (2013) Heterodimerization with its splice variant blocks the ghrelin receptor 1a in a non-signaling conformation: A study with a purified heterodimer assembled into lipid discs. *J. Biol. Chem.* 288, 24656–24665.
- (35) Koradi, R., Billeter, M., and Wuthrich, K. (1996) MOLMOL: A program for display and analysis of macromolecular structures. *J. Mol. Graphics* 14, 29–32, 51–55.